SHORELINE EXTRACTION USING LANDSAT-8 AND SENTINEL-2 IMAGES WITH SUBPIXEL PRECISION: A CASE STUDY IN BORACAY ISLAND, PHILIPPINES

Lizette Garalde[1],[1] Von Angelo Batingan[1], Roseanne Ramos*[2], Erica Erin Elazegui[1]
[1]Department of Geodetic Engineering, University of the Philippines Diliman, Quezon City, Philippines 1101
Email: llgaralde@up.edu.ph, vdbatingan@up.edu.ph, eeelazegui@up.edu.ph

[2]Assistant Professor, Department of Geodetic Engineering, University of the Philippines Diliman, Quezon City, Philippines 1101
* Email: rvramos@up.edu.ph

KEY WORDS: shoreline, subpixel precision, image registration

ABSTRACT: Accurate detection of shoreline contributes to understanding coastal environment behaviours and proper formulation of coastal zone development plans. The spatiotemporal variability of the land-water boundary poses a challenge to the proper delineation of shorelines. This study presents a methodology to detect instantaneous subpixel level shoreline from freely available satellite imagery of Landsat-8 and Sentinel-2. A combination of pansharpening methods, Modified Normalized Difference Water Index, Otsu's automatic thresholding, geostatistical techniques, and a subpixel level shoreline detection algorithm were employed to detect the fine morphological feature. Extracted features were registered to a high-resolution Kompsat-3 image using Discrete Fourier Transform, and were evaluated using Digital Shoreline Analysis System techniques. The implemented methodology displayed the ability to extract shoreline at subpixel precision and accuracy. The effect of tidal variations on image registration and overall accuracy was also analyzed. The subpixel algorithm was able to detect shoreline point approximates along a mesotidal beach in the Boracay Island, Philippines using images captured by Landsat-8 and Sentinel-2 that are smooth, continuous and with an overall subpixel precision of 8.61 m. The results exhibited the potential of the implemented methodology in integrating instantaneous subpixel shorelines extracted from Landsat-8 and Sentinel-2 and in allowing repetitive detection for coastal zone monitoring.

1. INTRODUCTION

A shoreline is defined as the edge of a body of water or the visible physical interface between land and water (Pascual et.al, 2012). Detection of shoreline contributes to understanding coastal zones that are considered a major socio-economic environment. Loss of life and property, among others, may occur when the shoreline is not properly identified (Aedla, et.al., 2015). Shoreline extraction is a fundamental study that can be used in several applications like coastline change detection and coastal zone management (Rasuly et.al., 2010). The observations in a similar study (Almonacid-Caballer et.al, 2016) show that mean shoreline, a coastal evolution indicator, can be produced from properly delineated shoreline positions. The creation of models for determining coastal erosion and accretion (Rasuly et.al., 2010), and coast's planimetric movement "hotspots" (Appeaning-Addo, 2009) would contribute to proper resource management and planning along the coastal area. Thus, coastal monitoring is essential to ensure national development and environmental protection (Aedla, et.al., 2015).

In Boracay Island in the Philippines, exposure to tourism-related activities and severe violations of environmental statutes accelerated the rate of coastal erosion. Easements were established to prevent damage to properties adjacent to water bodies. However, inconsistencies in reference lines used by government agencies in reckoning easements raised a conflict between residents and the local government of Boracay.

Multiple studies have used a pixel-based approach for the segmentation of the land-water boundary. However, pixel-based techniques remain confined to the dataset's spatial resolution while object-oriented classification would be less cost-effective on detecting shoreline on a regional scale, being more effective when classifying high-resolution images. In another related study (Pardo-Pascual, et.al, 2018), a shoreline approximation previously used on seawalls was applied to naturally-occurring micro tidal beaches. The temporal aspect of the study lead to variation in land cover spectral intensity that affected the extracted shorelines. To avoid such complications and address the fundamental problem on shoreline delineation, this paper aims to demonstrate the potential of integrating Landsat-8 and Sentinel-2 images using the proposed methodology for possible temporal shoreline analysis. The goals of the study are to integrate remote sensing

and geographic information systems (GIS) techniques for shoreline extraction on the mesotidal beach of Central Boracay and to evaluate the precision and accuracy of the extracted subpixel shorelines.

2. METHODOLOGY

2.1 Data Preparation

The medium resolution satellite images utilized in this study are Landsat-8 and Sentinel-2, with Kompsat-3 as reference image. The study area shown in Figure 1 is in Boracay Island, Malay, Philippines. It is located between geographic coordinates (11°56' N, 121°54' E) and 12°00' N, 121°57' E). Supplementary datasets include a Digital Elevation Model (DEM) of Boracay Island, and the tide table at the time of data acquisition of satellite images. The medium resolution satellite images were calibrated to surface reflectance images. A low pass filter was applied to optimize image registration with the down sampled reference image.

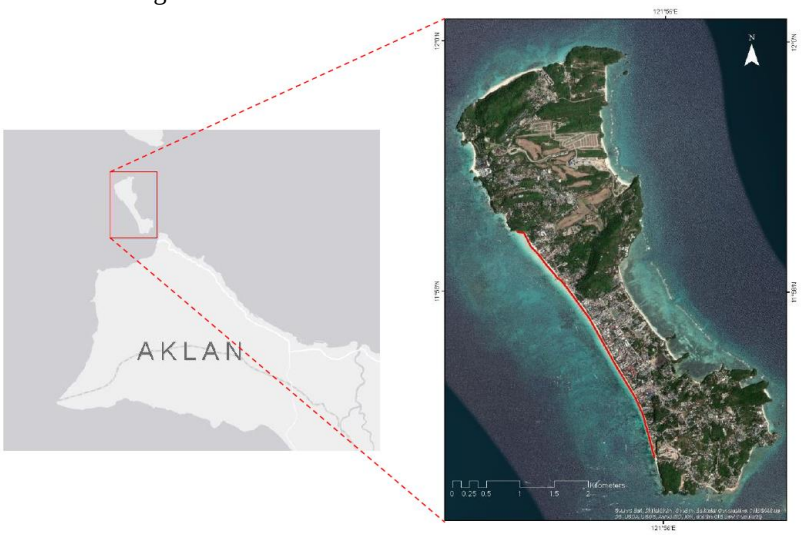

Figure 1. Study site (with coastline in red segment on the map) located in Boracay Island in Malay, Aklan, Philippines. Image Source © Google Earth, 2020

2.2 Shoreline Detection

The water index used for this methodology utilizes the green and Short-wave infrared (SWIR) bands of the medium resolution satellite data. These are bands 3 and 6 for Landsat-8 and Sentinel-2 bands 3 and 11. To improve the data's spatial resolution, Landsat-8 image was up sampled using Spectral Response Function Based (SRFB) weighted Intensity-Hue-Saturation (IHS) algorithm (Zhang and Roy, 2016) (Amro et.al, 2011). The unequal pixel resolution on Sentinel-2 bands 3 and 11 was addressed by employing the methodology developed in a previous study (Du et.al, 2016). Deemed better in image classification of water bodies, Modified Normalized Difference Water Index (MNDWI) (Xu, 2006) was used instead of utilizing infrared bands as observed from a related study (Pardo-Pascual, et.al, 2018). MNDWI images with a spatial resolution of 15-m and 10-m were produced for Landsat-8 and Sentinel-2, respectively. The MNDWI images were then binarized using Otsu's thresholding method (Otsu, 1979) to produce water/non-water maps. The extraction of the reference shoreline from Kompsat-3 was executed by creating a Normalized Difference Water Index (NDWI) image (Xu, 2006), then segmented with Otsu's technique to binarize the image. Focal statistics with Reclassify tool identified the pixels at the classified water body edge from the rest of pixels, forming the pixel-level shoreline for Landsat-8, Sentinel-2, and the reference image.

Based on another related study (Pardo-Pascual, et.al, 2018), the subpixel shoreline detection algorithm works under the assumption that the visible physical interface between land and water occurs where the MNDWI intensity gradient is maximum. This algorithm was expressed in a Python code with the pixel-lev el shoreline raster and the corresponding MNDWI image as input. For every classified pixel-level shoreline pixel, its corresponding pixel on the MNDWI image was identified, together with a 7x7 neighbourhood as shown in Figure 2a. In Figure 2b, each 7x7 MNDWI pixel neighbourhood was resampled to a 2.5-m increment neighbourhood using bilinear interpolation. Thus, a 42x42 and 28x28 resampled neighbourhood containing MNDWI values were obtained for Landsat-8 and Sentinel-2, respectively. Depending on the shoreline orientation duly identified, for every row/column on the interpolated neighbourhood, the pixel values were used as input for the polynomial curve fitting. The numerical coefficients of the polynomial function, $y=f(x)$ where y is the MNDWI value and x the corresponding resampled row/column, were approximated using non-linear least squares as shown in Figure 2c. Values that made the polynomial function's second derivative null were derived. The

root closer to the initial approximate, or the central column/row of neighbourhood, was chosen to be the location of the subpixel approximate on that resampled row/column. A Gaussian weight was assigned to each subpixel approximate identified under the assumption that a point is less accurate as it goes farther from the center of the analyzed neighbourhood.

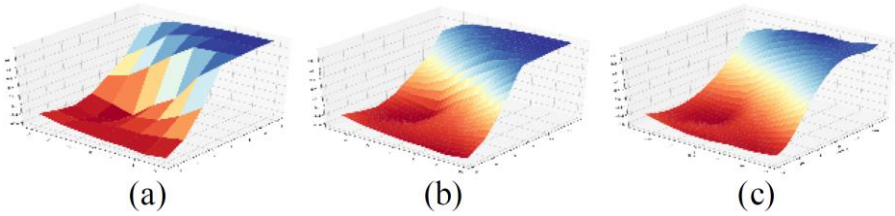

Figure 2. An illustration on the basic scheme of neighbourhood processing

Since the process was iterative and applied for every pixel on the pixel-level shoreline, the same pixel was processed on multiple instances producing multiple weighted solutions for the same area. The final position on a specific resampled row/column was then determined by the weighted average of the subpixel approximates as shown in Figure 3.

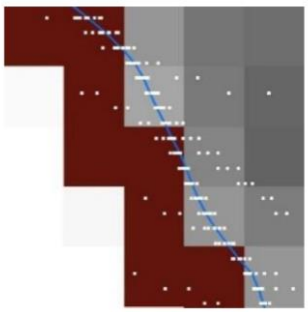

Figure 3. Shoreline position (blue) from multiple solutions (white) at each profile.

2.3 Image Registration and Georeferencing

The pre-processed Kompsat-3 image was used as the reference image, and the corresponding Landsat-8 and Sentinel-2 images were used as the target image. All images were clipped to the same extent to have the same dimensionality. The Near Infrared (NIR) bands of all images were used to calculate translation as it theoretically contained a greater change in reflectance between the sea and land (Pardo-Pascual, et.al, 2018). An up sampling factor of 100 was used to calculate the subpixel level translation values.

The shifts in pixels were then multiplied to the corresponding spatial resolutions of the target images to calculate the geometric displacements in meters. The point files obtained from the subpixel algorithm were translated using the shift values obtained from image registration. The translated shorelines were then converted to line features to be validated using Digital Shoreline Analysis System (DSAS) techniques.

3. RESULTS AND DISCUSSION

3.1 Shoreline

The shoreline delineated within the predetermined extent provided pixels that served as the initial approximate position of shoreline. Landsat-8 pixel-level shoreline obtained an approximate length of 6,405 m while Sentinel-2 obtained 5,380 m. The computed shoreline length from pixel approximation of Landsat-8 exceeded that of Sentinel-2 by roughly 1 km despite their area extent being roughly the same.

Finer shoreline was delineated on Sentinel-2, shown in Figure 4b, compared to Landsat-8 (see Figure 4a), due to its better spatial resolution. Further observation of the produced pixel shoreline of Landsat-8 revealed that the implemented methodology had classified multiple areas along the study area with cluster pixels as shoreline approximate. Unlike the Sentinel-2 data that had successfully separated parts within Boracay Island with water bodies, the spatial resolution of Landsat-8 did not allow consistent seawater and inland water separation. Thus, there is an excess of pixels that were classified using the Landsat-8 dataset. To provide context, the imposed easement on Boracay is 30 m. Hence, there exists a possibility that a Landsat-8 pixel that contains artificial water bodies set up by business establishments, which thrive along the shore, is in close proximity to a pixel that covers the shore and sea boundary. To implement the subpixel algorithm properly, the pixel-level shoreline of Landsat-8 was refined by declassifying pixel approximates that were

clustered around another shoreline pixel. The modified Landsat-8 pixel-level shoreline yielded an estimated shoreline length of 5,400 m which is closer to the approximated shoreline length of Sentinel-2, a percent difference of 0.37% for these estimated shoreline lengths.

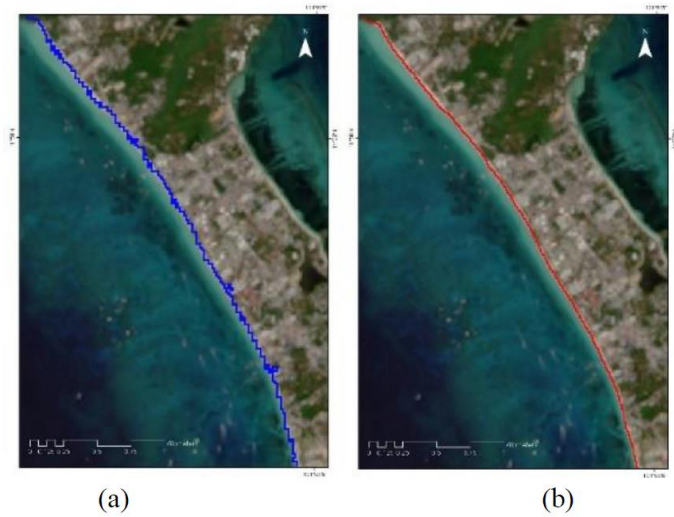

(a) (b)

Figure 4. Pixel-level shoreline overlaid on (a) Landsat-8 image and (b) Sentinel-2 image

The degree of polynomial curve used for the subpixel algorithm was determined by evaluating the variance between interpolated and curve fitted MNDWI values using R_2 scores. Between 3rd, 4th, and 5th polynomial degrees, the 4th degree, which obtained the highest R_2 mean score was used to implement the algorithm. The Python code bearing the subpixel algorithm was executed on a computer with the following specifications: Intel(R) Core(TM) i5-6200U CPU @ 2.30GHz, 64-bit operating system, 8 gigabytes RAM. The subpixel shoreline approximation took an average of 44.8 s for the whole area of interest. Connecting the resulting point approximates enabled the computation of the actual shoreline length, 5,480.33 m for Landsat-8, shown in Figure 5a, while 4,407.40 m for Sentinel-2 (see Figure 5b). This length value disparity can be inferred from the drastic sideway fluctuations on Landsat-8 subpixel shoreline that contributed to the total shoreline length.

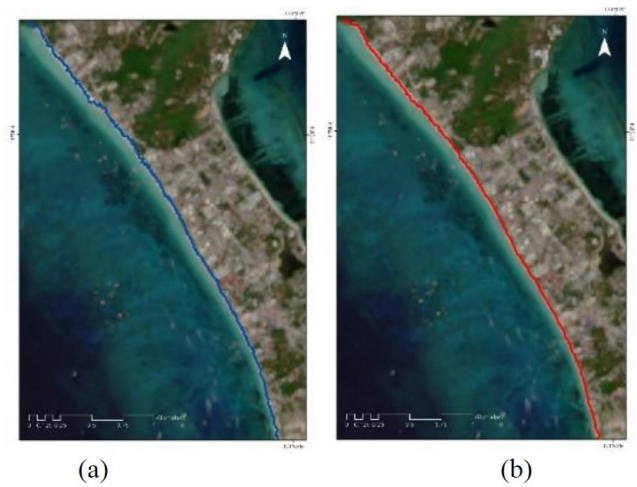

(a) (b)

Figure 4. Subpixel-level shoreline overlaid on (a) Landsat-8 image and (b) Sentinel-2 image

The performance of the subpixel approximation was inspected through measurement of the gaps between the point approximates extracted. Table 1 describes the morphology of the subpixel shorelines extracted wherein a lower value indicates smoothness. The 0.01 m difference between the datasets' mean ΔEastings values describes a general smooth trend of the subpixel shoreline. However, Sentinel-2 derived shoreline showed smoother structure evident in its lower standard deviation values. Thus, the integrity of the implemented methodology to detect the possible location of a fine, continuous, and smooth feature such as shoreline is exhibited. Furthermore, the positive sign on ΔEastings indicates that the shoreline leans landward or towards the east from top to bottom. The general orientation of shoreline in the study area is vertical; hence, the mean value for ΔNorthings both for Landsat-8 and Sentinel-2 is close to 2.5 m which is the predetermined spatial resolution of the neighbourhood resampling implemented on subpixel algorithm. The negative mean value of ΔNorthings describes the decreasing northings coordinate as the analysis of the shoreline went from top to bottom. The minimum and maximum gap values indicate the presence of large gaps between shoreline approximates.

These gaps were derived from the perturbation of the shorelines' shape caused by natural variables such as waves. Wave run-ups that leave the land wet at different time intervals may have affected the delineated feature. Referring to the slope map created from the 10-m DEM of Boracay, the relatively flat terrain that is evident on the upper part of the shoreline allowed run-ups, as shown in Figure 6a, to manifest on the subpixel shoreline extracted. In contrast, the lower part of the study area has a higher slope on the edge of the island; hence, run-ups were not easily distinguished in these parts, see Figure 6b.

Table 1. Disparity of Shoreline Point Approximates

Quantity	Mean ± standard deviation (m)	Max (m)	Min (m)
Landsat-8			
ΔEastings	1.47 ± 3.88	31.11	-12.06
ΔNorthings	-2.43 ± 1.06	12.41	-17.49
Distance	3.97 ± 2.91	32.20	2.08
Sentinel-2			
ΔEastings	1.48 ± 1.84	14.83	-5.31
ΔNorthings	-2.43 ± 0.77	4.38	-16.63
Distance	3.22 ±1.31	16.82	2.50

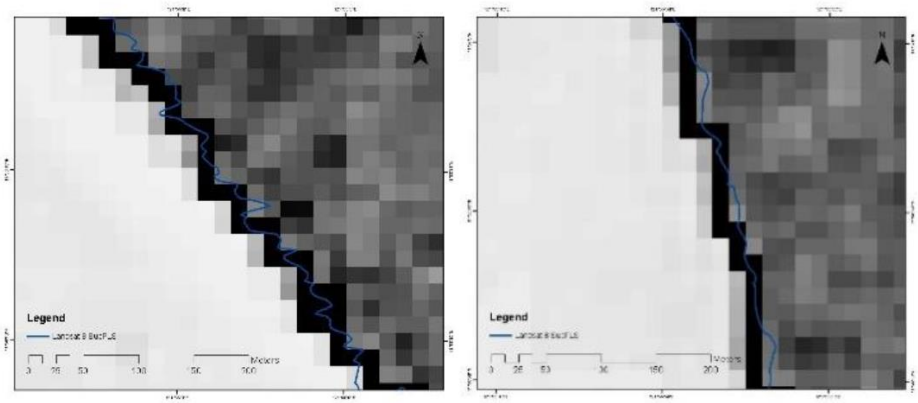

(a) (b)

Figure 6. Varying shoreline (in blue line) configuration in (a) wavy and (b) unwavy pattern

3.2 Subpixel precision and accuracy

The final translation *-dx* and *-dy*, was multiplied to the corresponding spatial resolution of the image. A -176.1 m horizontal and -2.2 m vertical displacement was applied to the Sentinel-2 extracted shoreline while the Landsat-8 shoreline obtained a -180.6 m and 7.2 m translation.

The displacement was initially expected to be at the subpixel level because both the reference and target images were already georeferenced and projected at the same coordinate system. However, the calculated displacements of the source images along the x-axis were high with the maximum value even reaching 180.6 m or 6 times the size of the corresponding pixel (30 m). The disparity can be inferred from the 50.99 m horizontal accuracy of the reference image at 90% Circular Error (K. Lee et.al, 2017).

The extracted shorelines were evaluated at 3 zones: Zone I, II, and III. The area was divided naturally due to the existence of seaports that were extracted from the high-resolution image (Figure 7). Reckoned from the reference shoreline, Zones I, II, and III are measured at 2.126 km, 2.359 km, and 1.027 km, respectively. Thus, an evaluation was performed on a 5.5 km long shoreline.

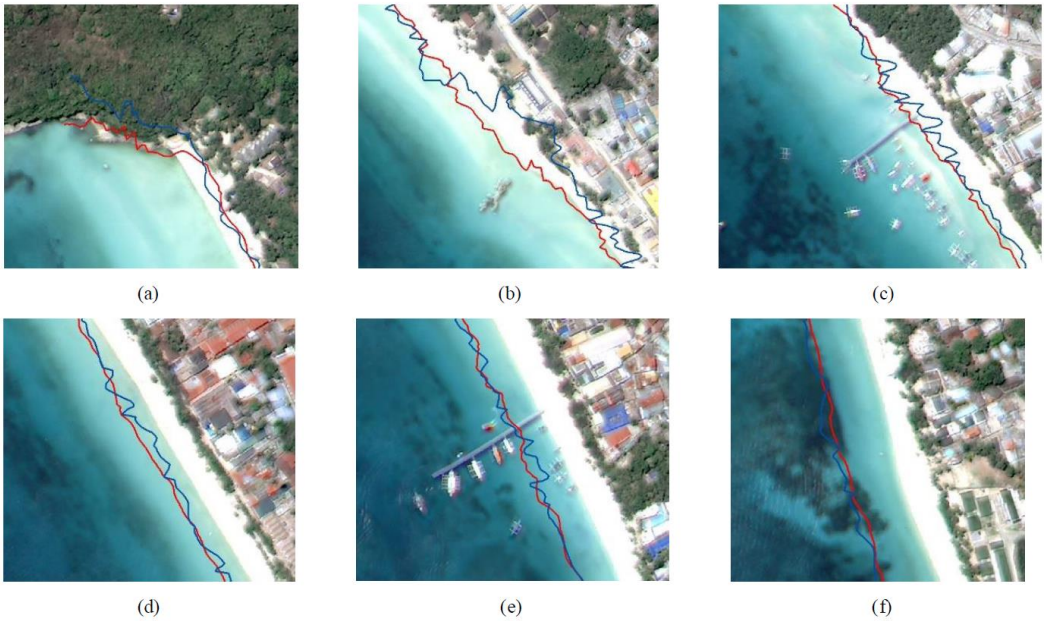

Figure 7. Georeferenced subpixel shoreline (blue line using Landsat-8, red line using Sentinel-2 image) assessed in different parts of the study site.

Table 2 shows the mean absolute distance (MAD) and standard deviation (SD) of the extracted shorelines from Landsat-8 and Sentinel-2 imagery for each sub-region. MAD refers to the mean absolute distance between the extracted shorelines at each transect. The transect was defined at a 2 m interval with a smoothing distance of 100. The length of the extracted Landsat-8 and Sentinel-2 shorelines were 5,480.33 m and 4,407.40 m, respectively, and a total of 2174 transects were created. Zone I had the lowest precision at 12.08 ± 10.01 m. This can be attributed to the existence of nonlinear Landsat-8 shoreline along Zone I whereas the corresponding area from Sentinel-2 achieved smoother lines. Composed of relatively straight shores, Zones II and III, however, achieved almost twice the precision of Zone I at 5.81 m and 7.02 m, respectively. Collectively, Table II shows that the shoreline extraction achieved subpixel precision at 8.61 ± 7.85 m which exhibits the potential of integrating Landsat-8 and Sentinel-2 images for extraction of shoreline to perform temporal shoreline analysis.

Table 2. Subpixel Shoreline Precision

Region	**Transect Count**	**Mean Absolute Distance ± standard deviation (m)**
Zone I	891	12.08 ± 10.01
Zone II	872	5.81 ± 4.17
Zone III	411	7.02 ± 5.18
All	2174	8.61 ± 7.85

The subpixel accuracy of the extracted Landsat-8 and Sentinel-2 shorelines were evaluated using the reference Kompsat-3 shoreline. As seen in Figure 8, the first two zones of Landsat-8, detected seaward values represented in shades of green were relatively closer to the true shoreline in comparison to landward values shown in red. Thus, as the majority of Zone I values are landward (91.26%), accuracy measured along the area remained relatively low at 14.92 m. This is due to the sinuous behavior of Landsat-8 subpixel shoreline along Zone I (see Figure 8a) as evident by its high MAD SD value of 10.03 m. In Zone II, the accuracy measured is highest at 11.00 ± 8.77 m and displays a seaward direction as seen in Figure 8b.

However, the subpixel extraction on Landsat-8 achieved an overall accuracy of 18.64 m due to the low accuracy achieved on Zone III at 44.52 m. For Zone III, despite the high precision of 7.02 m and seaward direction, the calculated accuracy was very poor wherein the values seen in shades of gray in Figure 8c even exceeded the pixel-level shoreline at 44.52 m. The disparity in the area, therefore, is irrelative to the extraction methods applied and can be attributed to the inherent difference between the reference and the extracted shoreline. However, despite the high MAD value, a low SD can be observed for Zone III which indicates that while the extracted subpixel shoreline is greatly displaced from the reference shoreline, its ability to reflect the true shape is unaffected.

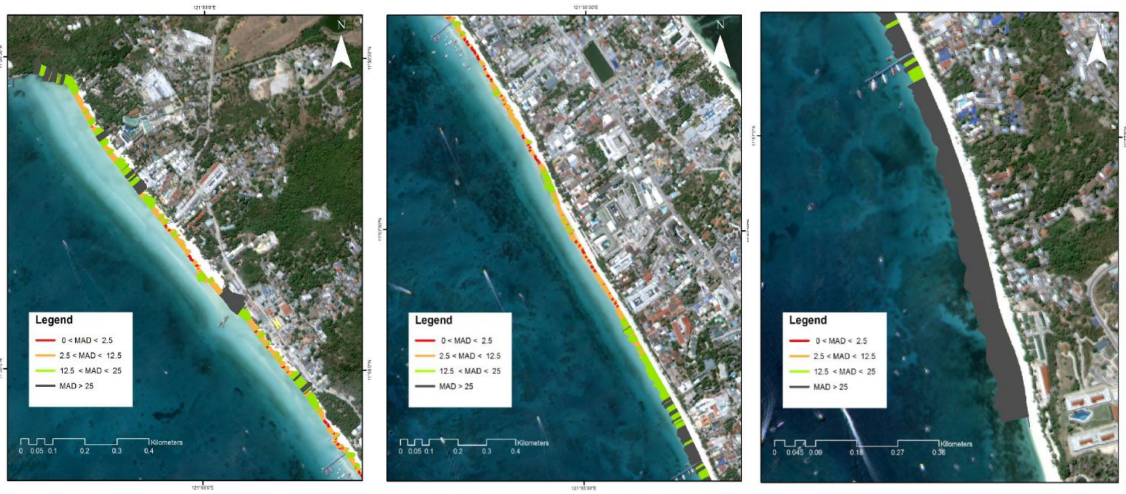

(a) (b) (c)

Figure 8. Shoreline extraction assessment using Landsat-8 image on (a) Zone I, (b) Zone II and (c) Zone III

In Figure 9, an opposite trend can be observed for the first two zones of Sentinel-2 wherein the landward offsets are closer to the true shoreline than seaward offsets. Zone I obtained the highest accuracy of 6.79 ± 4.87 m despite the low precision. This supports the earlier inference that the low precision along Zone I was due to the rough behaviour of the Landsat-8 shoreline. Figure 9a shows the smoothly extracted shoreline of Sentinel-2 along Zone I. Shoreline along with Zone II, obtained an accuracy of 13.01 m, which is notably lower than that of Landsat-8 shoreline. It can be observed from Figure 9b that the first half of the shoreline gained relatively higher accuracy but values slowly deviated and went to an extreme seaward direction for the second half which ultimately lowered the total accuracy along the second zone. However, in comparison to Landsat-8, lower MAD SD value for all zones can be observed for Sentinel-2 which implies smoother lines extracted and better replication of true shoreline shape. The seaward direction observed halfway of Zone II escalated to Zone III and the results along the area displayed similar behaviour to its Landsat-8 counterpart where it reflected relative shoreline shape (see Figure 9c) but the values obtained showed great offset from the true shoreline. Similarly, the 15.60 m overall accuracy obtained from Sentinel-2 derived shoreline was affected by low accuracy observed in Zone III at 39.79 m.

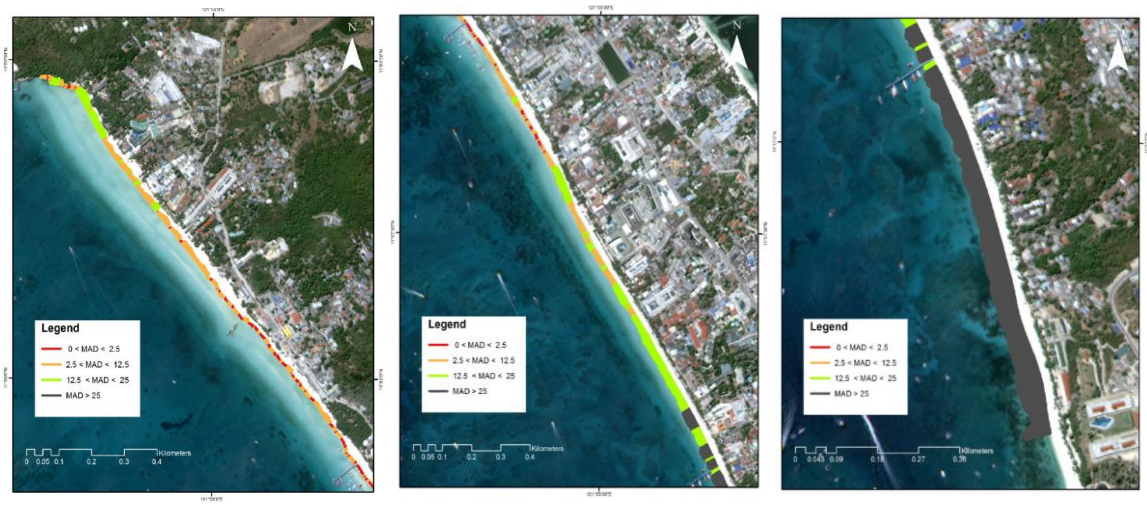

(a) (b) (c)

Figure 9. Shoreline extraction assessment using Sentinel-2 image on (a) Zone I, (b) Zone II and (c) Zone III

The disparity in accuracy obtained from Zone III compared to analogous values of Zone I and II cannot be attributed to the implemented extraction process. Other factors may contribute to the observed inconsistency. Considering the large difference in time acquisition of analyzed data, one of the most obvious natural factors that may directly affect the accuracy of shoreline delineated is the tide. It can be observed from the tide data that Kompsat-3 elevation is almost in the middle of intertidal range at that time, while the 13-minute gap on Landsat-8 and Sentinel-2 acquisition time has a

corresponding tidal elevation near the high tide. To derive a definite tide elevation at the time of the acquisition, an assumed linear behaviour with respect to time was used to compute the desired height that is existing at the obtained instantaneous scene. The computed tide elevation for Landsat-8, Sentinel-2 and Kompsat-3 are 1.39 m, 1.46 m, and 0.34 m, respectively. Using the 10-m slope map of Boracay, the average slope along each shoreline zone edge was obtained. The average slope is computed as the average of all slope pixel values that intersect the georeferenced subpixel shoreline for each dataset. The approximate shoreline planar shift is consequently computed as follows:

$$Planar\ Shift = \frac{\Delta tide\ elevation}{\tan \theta} \quad (1)$$

where $\Delta tide\ elevation$ is the difference between the tide elevations of reference image and Landsat-8 or Sentinel-2 and θ is the zonal average slope in degrees.

The slopes and the approximate shoreline location shift from Kompsat-3 intertidal situation to an almost high tide line on Landsat-8 and Sentinel-2 are shown in Table 3.

Table 3. Zone Slope and Tide-Induced Shift

	Landsat-8		**Sentinel-2**	
Region	**Slope (°)**	**Planar shift (m)**	**Slope (°)**	**Planar shift (m)**
Zone I	4.70	12.75	4.00	15.94
Zone II	3.35	17.89	3.35	19.04
Zone III	13.26	4.44	12.99	4.83

The displacement obtained through image registration considered this tidal variation due to the spectral values stored in the pixels. The values in georeferencing were obtained by shifting and matching scenes on high tide with the other experiencing intertidal condition. Thus, since the applied translation was generalized for the whole image and not for each zone, a 4 m to 5 m shift on shoreline location along Zone III was hardly considered compared to a more noticeable location shift on Zone I and Zone II shorelines. Generalizing the geolocation by applying a single *-dx* and *-dy* value throughout the length of subpixel shoreline, over shifted Zone III shoreline for both Landsat-8 and Sentinel-2. The excessive translation values made the Zone III shoreline absolutely seaward and ultimately caused the dramatic decline in the accuracy with respect to the reference shoreline.

Furthermore, the obtained planar shift values were not used to correct the translation values obtained from image registration for two reasons. First, these planar shifts are only an approximation for the tide-induced shoreline position shift because of the time acquisition disparity between the images and DEM. Tide elevations for each data were based only on the assumption of linear behaviour of tide elevation with respect to time and do not completely reflect the actual existing tide elevation at the instantaneous scene. Moreover, it is inappropriate to apply these obtained planar shifts to an extracted shoreline from an instantaneous scene because tidal variations are experienced gradually through time. Instead, the tide-induced error computed verifies the presence of natural errors that contributed to the validation results observed notably on Zone III. The presence of these natural errors, however, are expected when analyzing temporal data under the analysis' assumption that the extracted subpixel shorelines are at the same instant.

4. CONCLUSIONS

The integration of different remote sensing and GIS techniques enabled extraction of an approximate shoreline position. Utilization of multispectral data up sampling, water index, automatic thresholding, and geostatistical tools successfully obtained the Landsat-8 and Sentinel-2 approximate shoreline position at pixel level with a length percent difference of 0.37%. The implemented subpixel algorithm was able to detect shoreline point approximates along a mesotidal beach from Landsat-8 and Sentinel-2 that are smooth, continuous and with an overall subpixel precision of 8.61 m. The obtained precision quality by the delineated shorelines manifests the methodology's potential to combine Landsat-8 and Sentinel-2 archives on performing temporal shoreline analysis.

In this study, the utilization of a reference shoreline obtained from Kompsat-3 image validated the capacity of single-step DFT to obtain georeferenced shoreline that is of subpixel accuracy. The spatial resolution of original data greatly contributes to the performance of subpixel shoreline extracted from it. Nevertheless, both Landsat-8 (18.64 m) and Sentinel-2 (15.60 m) derived shoreline obtained an overall subpixel accuracy. Naturally-induced errors such as tidal variations that may affect the analysis should be considered. Minimum deviation on time of data acquisition is essential to avoid these uncontrollable factors. However, the obtained subpixel accuracy on both satellite images exhibits the potential of combining the subpixel shorelines extracted to be utilized for temporal analysis.

REFERENCES

Aedla, R., Dwarakish, G.S., Reddy, D.V., 2015. Automatic Shoreline Detection and Change Detection Analysis of Netravati-Gurpur Rivermouth Using Histogram Equalization and Adaptive Thresholding Techniques. Aquatic Procedia, vol. 4, pp. 563-570.

Almonacid-Caballer, J., Sánchez-García, E., Pardo-Pascual, J.E., Balaguer-Beser, A. A. and Palomar-Vázquez, J., 2016. Evaluation of annual mean shoreline position deduced from Landsat imagery as a mid-term coastal evolution indicator. Marine Geology, vol. 372, pp. 79-88.

Amro, I., Mateos, J., Vega, M., Molina, R., Katsaggelos, A.K., 2011. A survey of classical methods and new trends in pansharpening of multispectral images. EURASIP Journal on Advances in Signal Processing, 79 (2011).

Appeaning-Addo, K., 2009. Detection of Coastal Erosion Hotspots in Accra, Ghana. Journal of Sustainable Development in Africa, vol. 11 (4), pp. 253-265.

Du, Y., Zhang, Y., Ling, F., Wang, Q., Li, W., Li, X., 2016. Water bodies' mapping from Sentinel-2 imagery with Modified Normalized Difference Water Index at 10-m spatial resolution produced by sharpening the SWIR band. Remote Sensing, vol. 8 (4), 354. https://doi.org/10.3390/rs8040354

Lee, K., Kim, E., Kim, Y., 2017. Orthorectification of KOMPSAT Optical Images Using Various Ground Reference Data and Accuracy Assessment. Journal of Sensors, vol. 2017. https://doi.org/10.1155/2017/6393278

Otsu, N., 1979. A threshold selection method from gray-level histogram. IEEE Transactions on Systems, Man, and Cybernetics, vol. 9 (1), pp. 62-66. doi: 10.1109/TSMC.1979.4310076

Pardo-Pascual, J.E., Sánchez-García, E., Almonacid-Caballer, J., Palomar-Vázquez, J., de los Santos, E.P., Fernández-Sarría , A., Balaguer-Beser, A., 2018. Assessing the accuracy of automatically extracted shorelines on microtidal beaches from landsat 7, Landsat-8 and sentinel-2 imagery. Remote Sensing, vol. 10 (2), pp. 1-20. https://doi.org/10.3390/rs10020326

Pascual, J.E.P., Caballer, J.A., Ruiz, L.A., Vázquez, J.P., 2012. Automatic extraction of shorelines from Landsat TM and ETM+ multi-temporal images with subpixel precision. Remote Sensing of Environment, vol. 123, pp. 1-11.

Rasuly, A., Naghdifar, R., Rasoli M., 2010. Monitoring of Caspian Sea coastline changes using object-oriented techniques. Procedia Environmental Sciences, vol. 2, pp. 416-426.

Xu, H., 2006. Modification of normalised difference water index (NDWI) to enhance open water features in remotely sensed imagery. International Journal of Remote Sensing, vol. 27 (14), pp. 3025-3033. https://doi.org/10.1080/01431160600589179

Zhang, H., Roy, D., 2016. Computationally Inexpensive Landsat-8 Operational Land Imager (OLI) Pansharpening. Remote Sensing, vol. 8 (3), 180.